The Effect of SRP and Lunar Attraction on the Inclined MEO Satellite

Abdulrahman H. Saleh and Hind A. Ghanem
Department of astronomy and space, Collage of Science, Baghdad University, Baghdad, Iraq.

Abstract
In this paper some perturbations of a satellite orbit with heights more than 10000 km are studied. The two perturbations are due to the presence of other gravitational bodies such as Moon as a conservative perturbing forces and from the non-conservative perturbing forces such as SRP for satellite with A=5.1 m^2 and m=900 kg. The position, velocity and momentum components are calculated for the perturbed equation of motion at any instant of time and thus calculate the orbital elements of each perturbation. The orbital elements for the perturbed orbit will deviate from initial elements with time. The equations of motion solved numerically using the fourth order of Runge Kutta method. The results show that the secular variation for orbital elements are true but very small.

Keywords: Orbit, Solar radiation pressure, Lunar attraction.

تأثير ضغط الإشعاع الشمسي وجذب القمر على الأقمار الصناعية الأرضية المائلة المتوسطة الارتفاع

عبد الرحمن حسين صالح و هند عوني غانم
قسم الفلك والفضاء، كلية العلوم، جامعة بغداد، بغداد، العراق

الخلاصة:
تم في هذا البحث دراسة تأثير بعض الاضطرابات في مدار القمر الصناعي للارتفاعات الأكثر من 10000كم اضطرابات جذبية كجذب القمر واضطرابات غير جذبية كضغط الإشعاع الشمسي مع اعتبار مساحة القمر الصناعي 5.1 م^{2}وكتلته 900 كيلوغرام . حيث تم حساب إحداثيات الموضع والسرعة والزخم للقمر الصناعية خلال أي لحظة زمنية من معادلة الحركة المضطربة وبالتالي حساب العناصر المدارية لكل اضطراب . وجد أن العناصر المدارية للمدارات المضطربة سوف تنحرف عن قيمها الابتدائية . معادلة الحركة تم حلها عدديا باستخدام طريقة رانج كوتا للمرتبة الرابعة . النتائج تبين أن التغير على مدى عدة دورات للعناصر المدارية هو حقيقي لكنه صغير نسبيا.

Introduction

The satellite orbits are classified as many types according to height and inclination as well as the aims of the satellite work. The Earth and satellite are two body in space moving around the center of mass which is consider on the center of the Earth where mass of the earth $M_e \gg m_{sat}$ mass of satellite there are many effects on the satellite orbit by the other body in space or by solar radiation, these effect call a perturbations as the following survey:

Kozai (1959) developed the main secular and long-period terms of the disturbing function due to the lunisolar perturbations in terms of the orbital elements [1]. Musen (1960) derived first order expressions for the rates of change in the osculating elements caused by the direct Solar Radiation Pressure (SRP) [2]. This research

*Email: hindawny_89@yahoo.com

would be later expanded by Musen, Bailie and Upton (1961) to include the Paralactic term in the disturbing function [3]. Kozai (1961) developed the main secular and long period terms of the disturbing function due to the lunisolar perturbations in terms of the orbital elements of the satellite [4]. Kaula (1962) developed the Lunar and Solar disturbing function for a close satellite and developed a quasi potential for the radiation pressure effects to be used in the equation of motion. He did not obtain the solution [5]. Radzievskii and Artem've (1962) studied the influence of SRP on the motion of artificial Earth satellites [6].
Adams, Jr., and Hodge(1965) calculated the effect of SRP on orbital eccentricity[7]. Sehnal (1975) discussed the direct SRP, as one of the non-gravitational forces, from all its different aspects [8]. Anselmo, Bertotti, Farinella, Milani and Nobili (1983) had analyzed the perturbations due to SRP, only, on the orbit of a high artificial satellite [9]. Buffet (1985) studied the perturbations of orbital elements of the GPS satellites [10]. Broucke (1992) developed the general form of the disturbing function of the third body which was truncated after the term of second order in the expansion of Legendre polynomials [11]. Toshihiro Kubo-oka and Sengoku (1999) developed a radiation pressure model of the relay satellite (SELENE). Radiation forces acting on each part of the spacecraft were calculated independently and summed vector to obtain the mean acceleration of the satellite center of mass [12]. Su (2000) studied the GEO, MEO satellites and like GPS, GLONAS [13].

The effect of the third body perturbation by Solórzano and Prado (2004), (2007),Costa and Prado (2010) ,Lara , San-Juan , López and Cefola (2012), Rahoma and Metris (2012) [14,15,16,17]. Bar-Sever and Kuang (2005) introduced a set of solar pressure models for GPS satellites based on orbit tracking data [18]. Eshagh and Najafi (2007) evaluated the perturbations in orbital elements of a low earth orbiting satellite [19]. Valk and Lemaître (2008) investigated the long-term perturbations of the orbits of geosynchronous space debris influenced by direct radiation pressure including the Earth's shadowing effects [20]. Kezerashvili and V´azquez-Poritz (2009) studied SRP affects the period of the satellite and considered deviations from Keplerian orbits[19].McMahon and Scheeres (2010) analyzed the Secular orbit variation due to solar radiation effects [20]. Khalil and Ismail (2011) studied the effects of radiation pressure and Earth's oblatness on high altitude artificial satellite orbit[22]. Sun, Zhao, Zhang and Hou (2013) discussed dynamical evolution of high area-to-mass ratio objects in Molniya orbits[25].

The aim of this work is calculation the variation of orbital elements due to solar radiation pressure and lunar gravity for the medium Earth orbit of satellites at different heights with inclination (63^{o}) and eccentricity(0.1) through twenty periods.

The satellite orbit and solution

In celestial mechanics one is concerned with the motions of celestial bodies under the influence of mutual mass attraction. The simplest form is the motion of two bodies (Two-body problem). For artificial satellites the mass of the smaller body (satellite) usually is neglected, compared with the mass of the central body (the Earth).

Under the assumption that the mass distribution of bodies is homogeneous, and thus generates the gravitational field effect of a point mass the orbital motion for the two-body problem can be described empirically by Kepler's laws and can also be derived analytically from Newtonian Mechanics [25].
The mean motion (n) written as[26] ,

$$n = \sqrt{\frac{\mu}{a^3}} \quad , \qquad (1)$$

where:

$\mu = G(M + m)$,
$G = 6.67259\times10^{-11}\, m^3 kg^{-1} S^{-2}$ is the gravitational constant, M and m are the masses of the
Earth and satellite respectively.

The mean anomaly in any time which used to describing the location of the satellite in an orbit

$$M_{i+1} = M_i + n \times \Delta t \quad , \qquad (2)$$

And the eccentric anomaly for the orbit calculated as

$$E = M + e^{*} \sin E \quad , \qquad (3)$$

where

$$e^{*} = e \times \frac{180}{\pi}$$

This equation is called Kepler equation, although its looks as simple equation but its

solved by using numerical methods(iterative) , and one of these formulas which gives an approximate results can be found by following equation in ref. [27]:

$$E_{i+1} = E_i - \frac{E_i\, e\, \sin E_i - M}{1 - e\, \cos E_i}$$

To find the Cartesian coordinate (x_w and y_w) to the satellite in its orbit

$$x_w = a(\cos E - e)$$

$$y_w = a\sqrt{1-e^2}\,\sin E$$

$$z_w = 0$$

and the displacement radius (r) will be

$$r = a(1 - e\cos E) \qquad (4)$$

By direct differentiation for (x_w and y_w) one obtains

$$\dot{x}_w = \frac{\sqrt{\mu a}}{r}\sin E$$

$$\dot{y}_w = \frac{\sqrt{\mu a\,(1-e^2)}}{r}\cos E$$

$$\dot{Z}_w = 0$$

$$\dot{r} = \frac{\sqrt{\mu a}}{r}\, e \sin E \qquad (5)$$

The conversion of position and velocity of the satellite from this orbital plane to the Earth equatorial plane can be utilized by Gaussian vector (conversion matrix), which content Euler angle (i, Ω, ω) .

$$\begin{bmatrix} x \\ y \\ z \end{bmatrix} = R^{-1} \begin{bmatrix} x_w \\ y_w \\ z_w \end{bmatrix}$$

where R^{-1} is the inverse of Gauss matrix

$$R^{-1} = \begin{bmatrix} P_x & Q_x & W_x \\ P_y & Q_y & W_y \\ P_z & Q_z & W_z \end{bmatrix}$$

Thus the position components:

$$x = P_x x_w + Q_x y_w + W_x z_w$$
$$y = P_y x_w + Q_y y_w + W_y z_w$$
$$z = P_z x_w + Q_z y_w + W_z z_w$$
$$r = (x^2 + y^2 + z^2)^{1/2} \qquad (6)$$

And the velocity components:

$$\dot{x} = P_x \dot{x}_w + Q_x \dot{y}_w + W_x \dot{z}_w$$
$$\dot{y} = P_y \dot{x}_w + Q_y \dot{y}_w + W_y \dot{z}_w$$
$$\dot{z} = P_z \dot{x}_w + Q_z \dot{y}_w + W_z \dot{z}_w$$
$$\dot{r} = (\dot{x}^2 + \dot{y}^2 + \dot{z}^2)^{1/2} \qquad (7)$$

The basic equation of satellite motion is

$$\ddot{r} = -\frac{\mu}{r^3}\,\vec{r} \qquad (8)$$

Perturbed orbits and solutions

To distinguish perturbed forces from the central force (central body acceleration) these are generally referred to as perturbing forces. The satellite experiences additional accelerations because of these forces, which can be combined into a resulting perturbing acceleration vector $\ddot{r}_p$. The extended eqautions of motion are[28]:

$$\ddot{r} = -\frac{\mu}{r^3}\,\vec{r} + \ddot{r}_p \qquad (9)$$

Perturbing forces are in particular responsible for:

1. Accelerations due to the non-spherically and inhomogeneous mass distribution within Earth (central body), $\ddot{r}_E$.
2. Accelerations due to other celestial bodies (Sun, Moon and planets), mainly $\ddot{r}_S$, $\ddot{r}_M$.
3. Accelerations due to Earth and oceanic tides, $\ddot{r}_e$, $\ddot{r}_o$.
4. Accelerations due to atmospheric drag, $\ddot{r}_D$.
5. Accelerations due to direct and Earth-reflected solar radiation pressure, $\ddot{r}_{SP}$, $\ddot{r}_A$.

$$\ddot{r}_p = \ddot{r}_E + \ddot{r}_S + \ddot{r}_M + \ddot{r}_e + \ddot{r}_o + \ddot{r}_D + \ddot{r}_{SP} + \ddot{r}_A$$

Integration of Equation (9) by using numerical integration method and the six variables required from equation (9) are composed of three positional components and three velocity components. The fourth-order Runge Kutta method has been used here to find the accurate components of position and velocity which are used to calculate the new elements for the perturbed orbit.

The solar radiation pressure

The Sun emits a nearly constant amount of photons per unit of time. At a mean distance of 1 A.U. from the Sun, this radiation pressure is characterized as a momentum flux having an average value of $4.56\times10^{-6} N/m^2$ [29].

The effect of solar radiation pressure on satellite orbit can be divided into two categories, i.e. direct radiation and earth albedo radiation. Because MEO satellites are much far away from the earth surface, the earth albedo radiation has small influence on this type of satellites and can be neglected. Therefore only the direct radiation

pressure should be considered in the satellite dynamic models [13].

The solar radiation pressure is inversely proportional to the mass of the satellite. If the satellite is light and large then it is more affected. If the satellite is heavy and small it is less affected by the solar radiation. The satellite is constructed of materials with different refectories therefore modulation of such perturbation is very complicated, solar radiation pressure can be written as[19,29]:

$$\ddot{r}_{SP} = -p(1+\eta)\frac{A}{m}\nu\hat{u} \qquad (10)$$

where,
p is momentum flux,
η is reflectivity coefficient of the area A,
A is cross-sectional area of the satellite normal to the Sun,
m is satellite mass,
ν is the eclipse factor (1 being full Sun, 0 being full shadow),
$\hat{u}$ is the unit vector pointing to the Sun from the satellite.

As it can be seen from the Equation(10) the perturbation depends on different parameters and most of these parameters are not easy to determine. The momentum flux varies with time and cannot be estimated easily. Reflectivity of the coating used is not easy to determine and changes with time as the material wears out. The attitude of the spacecraft will impact the cross-sectional area that is exposed to solar radiation. And finally the calculation of the eclipse factor (ν) can be challenging for many orbits[25].In this work the inclination used is 63° where no eclipse therefore $\nu = 1$ all ways and $\frac{A}{m}$ For most satellite is less than 0.02.

Lunar gravity

The effects of the Moon will be treated as a third body acting on the satellite. Although the mass of the Moon is much lower than that of the Sun the reduced distance between perturbing body and satellite makes the Lunar perturbation about equal to the Solar [30].

$$\ddot{r}_M = \frac{\mu_l r}{r_l^3}[3(i_r . i_l)i_l - i_r] \quad , \quad (11)$$

where
$\mu_l = GM_l = 4.902794 \times 10^3 \ (N.Km^2/Kg)$
r_l radial distance between center of Moon and Earth .
i_l unit vector of the distance between centre of Moon and Earth.
i_r unit vector of the distance between Satellite and centre of Earth .
The relationships between the vectors used in this equation are illustrated in figure (1).

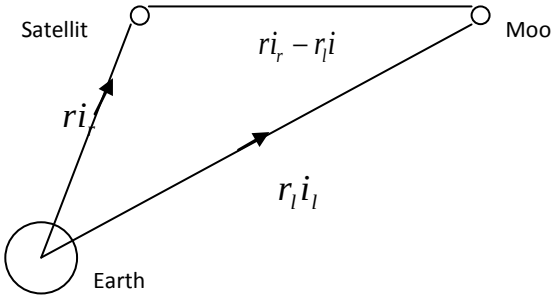

Figure 1- Lunar gravity geometry .

The biggest problem is calculating the Moon's position at a given point in time. And The empirical relationships to calculation Moon's position quoted from Meeus [31].

Calculating the orbital elements

The elliptical orbital elements in general are (i, Ω, ω, a, e, M) can be calculated from the component of position, velocity and angular momentum as follows [26] :

The inclination (i) of the orbit from the equatorial plane is given by

$$\tan i = \frac{\sqrt{h_x^2 + h_y^2}}{h_z} \quad , \quad (12)$$

The longitude of ascending node (Ω) is calculated as :

$$\tan \Omega = \frac{h_x}{-h_y} \quad , \quad (13)$$

the semi-major axis of the orbit calculated as:

$$a = \left(\frac{2}{r} - \frac{v^2}{\mu}\right)^{-1} \quad , \quad (14)$$

For elliptic orbits a will always be positive. The eccentricity (e) of the orbit is calculated as :

$$e = \sqrt{1 - \frac{h^2}{\mu a}} \quad , \quad (15)$$

The eccentric anomaly (E) is calculated as :

$$\tan E = \left(\frac{1 - \frac{r}{a}}{x\dot{x} + y\dot{y} + z\dot{z}}\right)\sqrt{a\mu} \quad , \quad (16)$$

The mean anomaly (M) is calculated as:

$$M = E - \frac{x\dot{x} + y\dot{y} + z\dot{z}}{\sqrt{a\mu}} \quad , \quad (17)$$

The true anomaly (f) is calculated as :

$$\tan f = \frac{\sqrt{1-e^2}\sin E}{\cos E - e} \quad , \quad (18)$$

The argument of the latitude (u) is calculated as

$$\tan u = \frac{zh}{-xh_y + yh_x} \quad , \quad (19)$$

The argument of perigee (ω) can be found as **:**

$$\omega = u - f \quad . \quad (20)$$

The programs are designed as the following steps

1. Calculation of the Julian date at perigee of orbit and the time of period .
2. Choosing the initial elements of orbit and the time step.
3. Calculation of the position and velocity of satellite by solving kepler's equation by using Newton Raphson's method .
4. Calculation of the central acceleration and the accelerations of solar radiation pressure perturbation and lunar attraction perturbation .
5. Solution the perturbed equation of motion by using fourth order Runge-Kutta method trough time T/100 to find the accurate position and velocity components.
6. Calculation of the satellite orbital elements due to each perturbation through 20 periods.

The input data for MEO altitudes are h=10000, 20000,30000 (km) with e= 0.1, i= 63 deg, Ω= 30 deg, ω= 40 deg where the semi major axis of the orbit is calculated as :

$$a = \frac{r_p}{(1-e)} \quad , \quad (21)$$

where

$$r_p = h_p + R_e = h_p + 6378.165\,Km \quad , \quad (22)$$

And the period calculation by kepler's 3th law

$$T = 2\pi\sqrt{\frac{a^3}{\mu}} \quad . \quad (23)$$

Results and Discussion

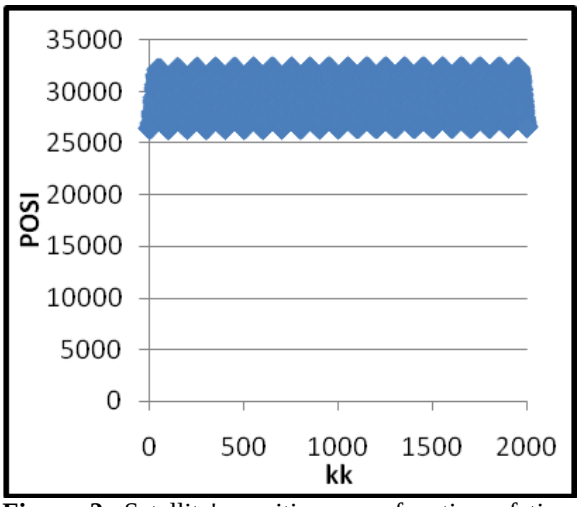

Figure 2- Satellite's position as a function of time during 20 period at hp=20000km.

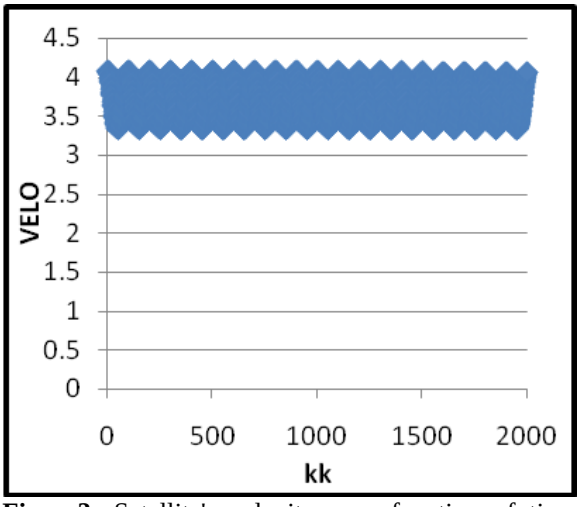

Figure3- Satellite's velocity as a function of time during 20 period at hp=20000km.

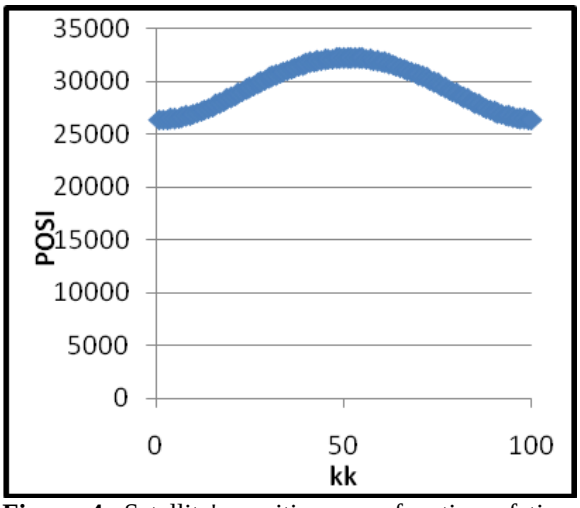

Figure 4- Satellite's position as a function of time during one period at hp=20000km.

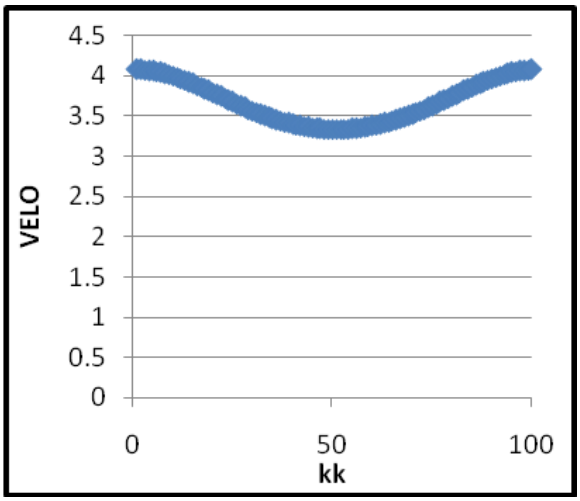

Figure5- Satellite's velocity as a function of time during one period at hp=20000km.

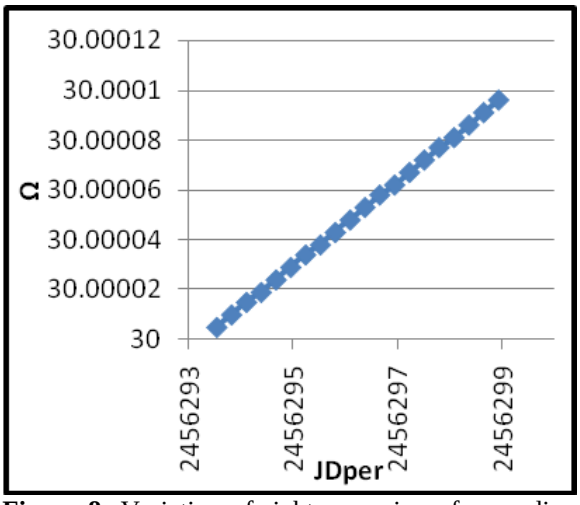

Figure 8- Variation of right ascension of ascending node with time due to SRP at hp=10000km, i=63°.

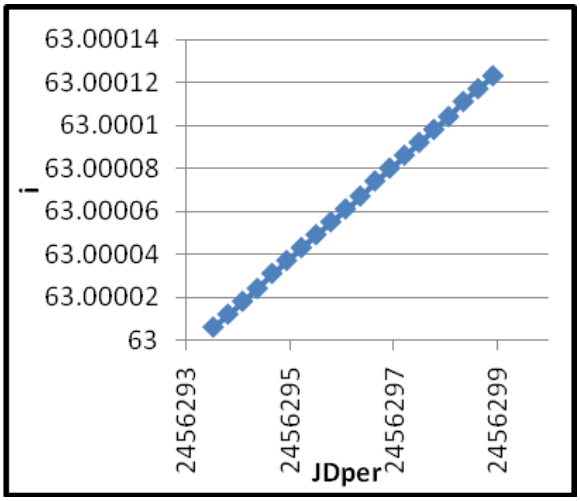

Figure6- Variation of inclination with time due to SRP at hp=10000km,i=63° .

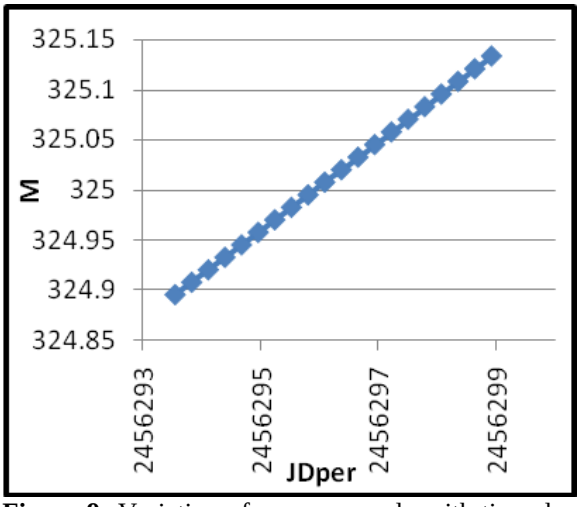

Figure 9- Variation of mean anomaly with time due to SRP at hp=10000km,i=63°.

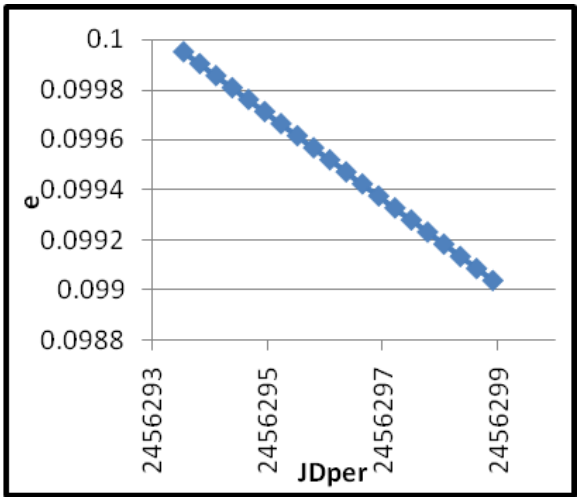

Figure7- Variation of eccentricity with time due to SRP at hp=10000km,i=63° .

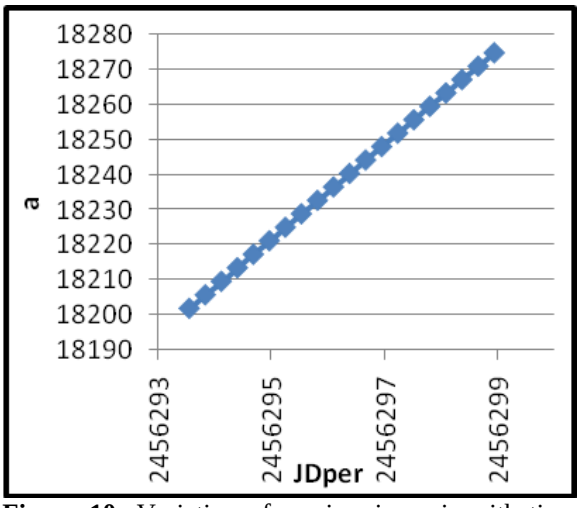

Figure 10- Variation of semi-major axis with time due to SRP at hp=10000km,i=63°.

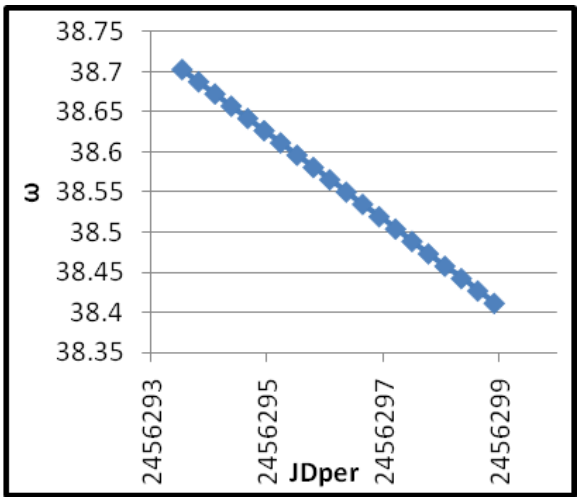

Figure 11- Variation of argument of perigee with time due to SRP at hp=10000km , i=63°.

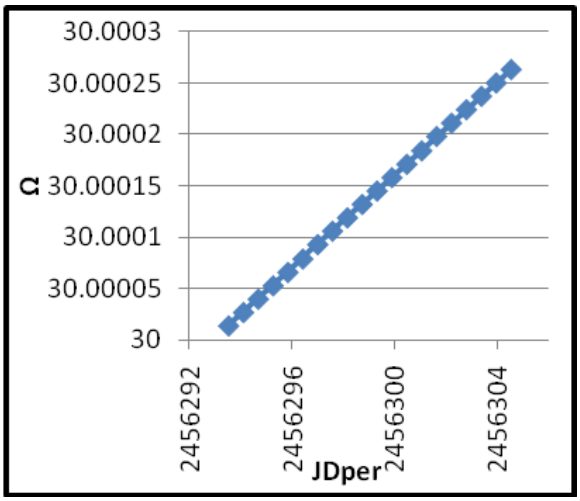

Figure 14- Variation of right ascension of ascending node with time due to SRP at hp=20000km, i=63°.

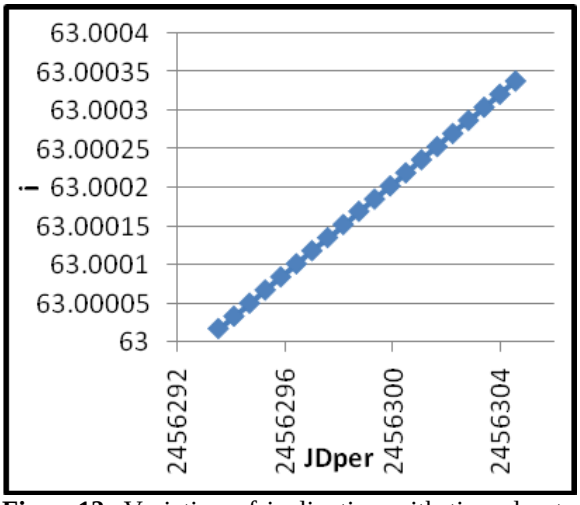

Figure12- Variation of inclination with time due to SRP at hp=20000km,i=63° .

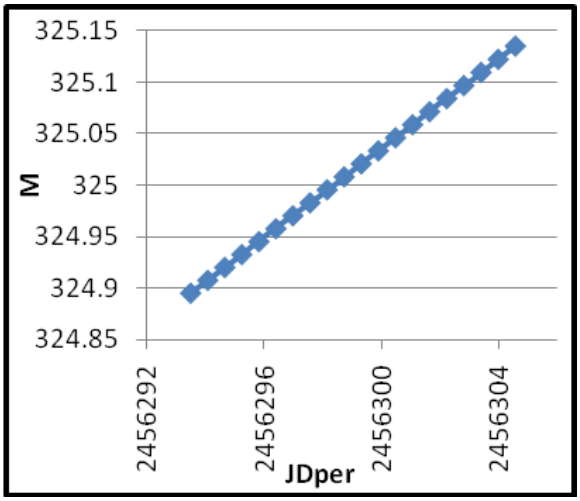

Figure 15- Variation of mean anomaly with time due to SRP at hp=20000km,i=63°.

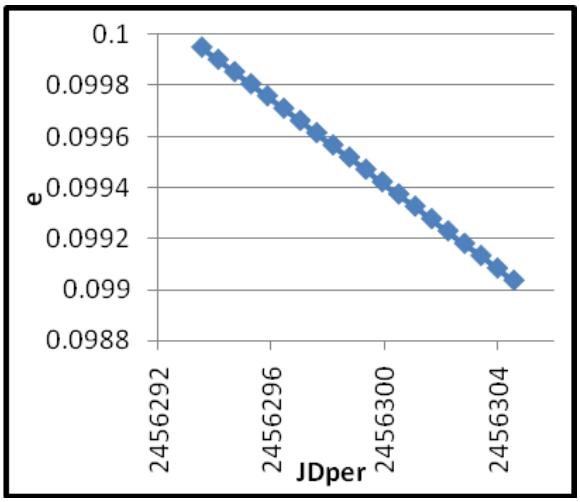

Figure13- Variation of eccentricity with time due to SRP at hp=20000km,i=63°.

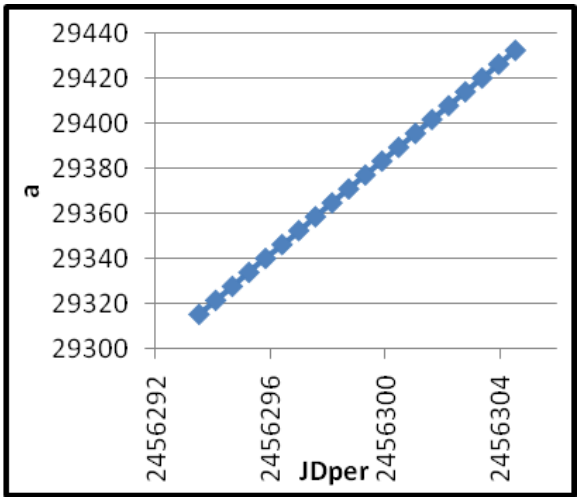

Figure 16- Variation of semi-major axis with time due to SRP at hp=20000km,i=63°.

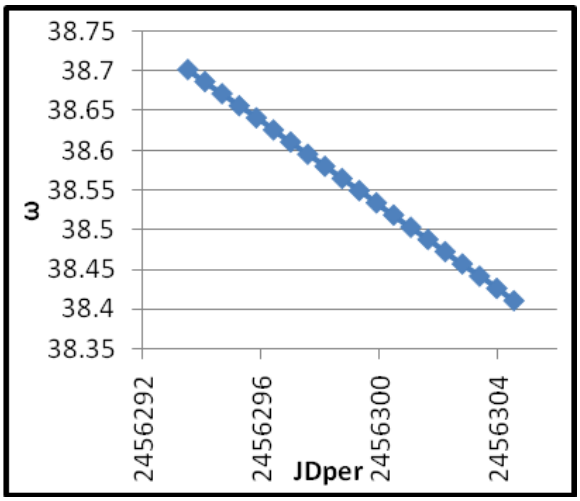

Figure 17- Variation of argument of perigee with time due to SRP at hp=20000km, *i*=63°.

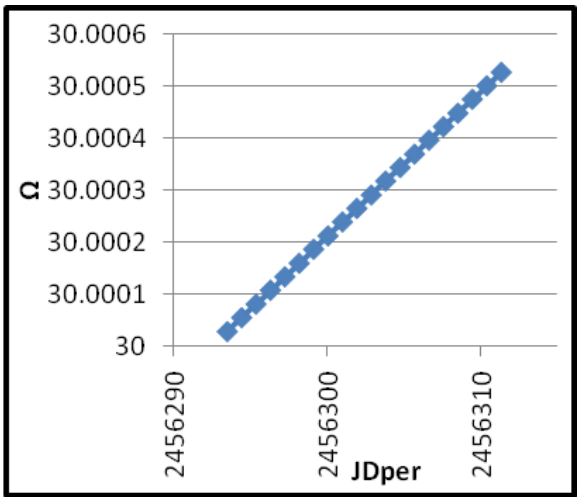

Figure20- Variation of right ascension of ascending node with time due to SRP at hp=30000km, *i*=63°.

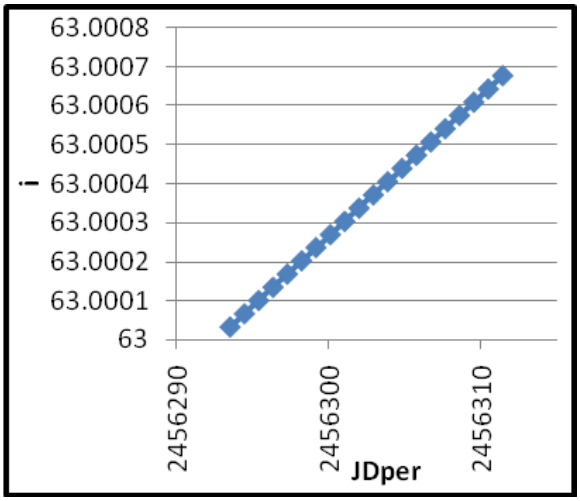

Figure18- Variation of inclination with time due to SRP at hp=30000km,*i*=63°.

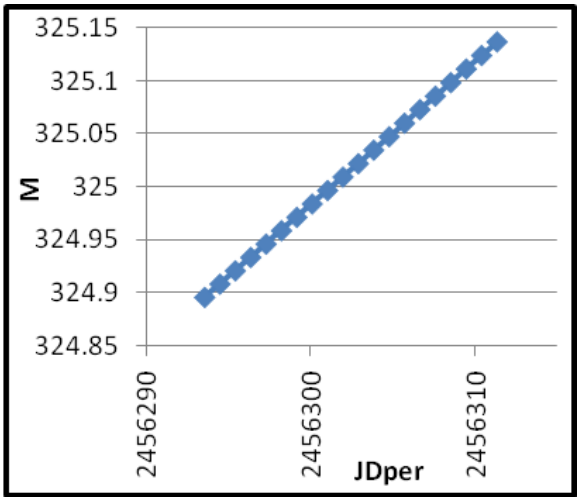

Figure21- Variation of mean anomaly with time due to SRP at hp=30000km,*i*=63°.

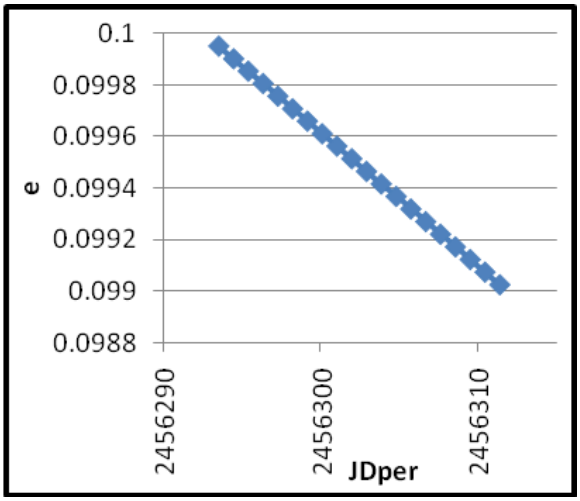

Figure19- Variation of eccentricity with time due to SRP at hp=30000km,*i*=63°.

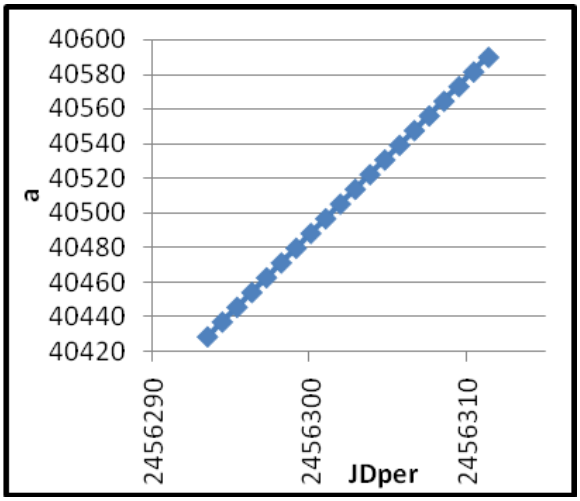

Figure22- Variation of semi-major axis with time due to SRP at hp=30000km,*i*=63°.

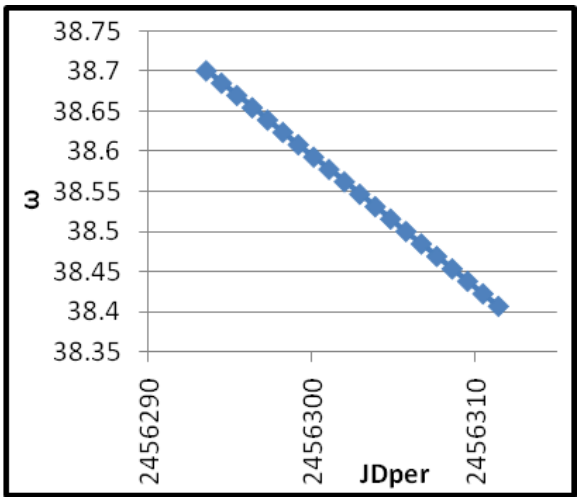

Figure23- Variation of argument of perigee with time due to SRP at hp=30000km, i=63°.

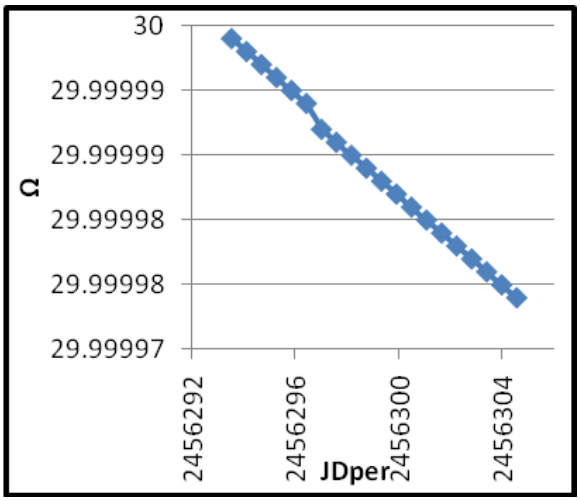

Figure 26- Variation of right ascension of ascending node with time due to lunar attraction at hp=20000km, i=63°.

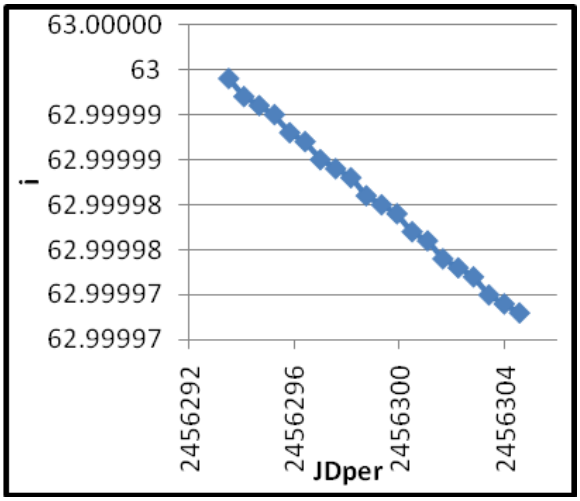

Figure 24- Variation of inclination with time due to lunar attraction at hp=20000km, i=63° .

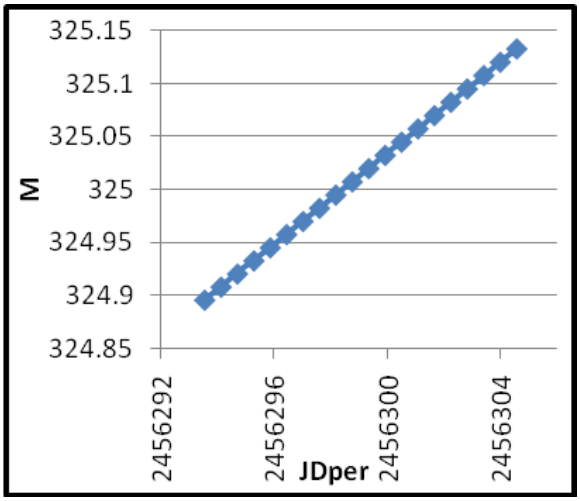

Figure 27- Variation of mean anomaly with time due to lunar attraction at hp=20000km, i=63°.

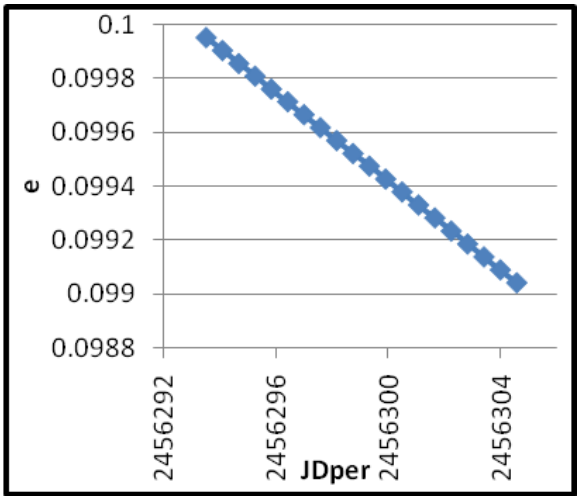

Figure 25- Variation of eccentricity with time due to lunar attraction at hp=20000km, i=63°.

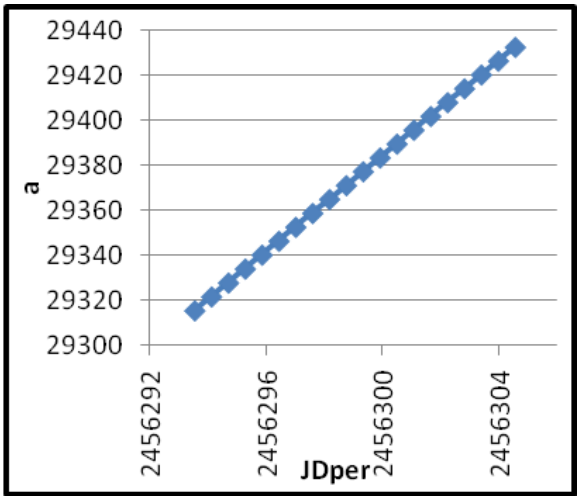

Figure 28- Variation of semi-major axis with time due to lunar attraction at hp=20000km, i=63°.

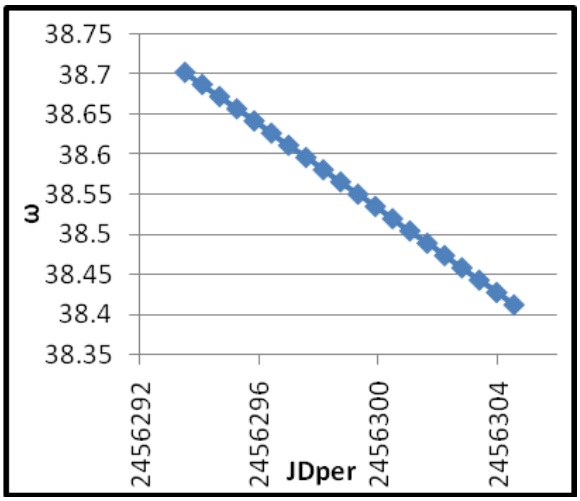

Figure 29- Variation of argument of perigee with time due to lunar attraction at hp=20000km, i=63°.

The results of our program are tested with some references and show a good agreement and discussed as the following :

Figures (2,3)shows that the periodic variation in position and velocity of satellite without perturbation through 20 periods at hp =20000 km and figures (4,5) illustrate the change in position and velocity through one period between perigee (r = 26378.165 km , v= 4.077 km/sec) and apogee (r = 32239.980 km , v = 3.336 km/sec) these values are suitable .

Figures (6,12,18)and (8,14,20) shows the secular variation of inclination and right ascension of ascending node due to SRP for altitudes hp = 10000, 20000, 30000 (km) where the values of it increases with time. The inclination variation is (Δi= 1.000001952380952 , 1.000005365079365, 1.000010761904762 deg) and the variation of right ascension of ascending node ($\Delta\Omega$ = 1.0000032, 1.000008766666667, 1.0000176 deg) through 20 periods .

Figures (10,16,22) shows that the semi major axis (a) at hp=10000, 20000 , 30000 (km) increases with time . The change is secular and it remains constant through any one rotation .

Semi major axis during 20 rotations increases with increasing altitude and the variations (Δa = 1.004220943520906, 1.004215375687233, 1.004204074916624 km).It is observed that the magnitude of perturbation at hp=30000 larger than its values at hp=10000,20000.

Figures (7,13,19)shows that the eccentricity (e) decreases with time. The change is similar at altitudes hp=10000, 20000, 30000(km) (Δe=0.99952) and the variation is secular through 20 periods .

Figures (9,15,21) shows the secular variation in mean anomaly (M) for altitudes hp=10000, 20000, 30000 (km) through 20 periods and mean anomaly at the perigee increases with time. That means the perigee is changing and return back.

Figures (11,17,23) shows the secular behavior of argument of perigee that decreases with time where($\Delta\omega$=0.9675578,0.967551775,0.967544475deg) .

Figures (24,26) shows the Lunar attraction effect and the secular variations in inclination and right ascension of ascending node for altitude hp=20000 (km) that decreases with time through 20 periods, the variation is(Δi= 0.9999999841269841deg) and ($\Delta\Omega$= 0.9999999666666667 deg).

Inclination of Moon changes from the highest value 28° to the lowest value -28° where the satellite's inclination 63° in all cases, makes the effect of the moon on the satellite always similar to that in this direction will cause a decrease in values of inclination and right ascension of ascending node of satellite.

As well as for the sun's influence will be constantly increasing because the sun's inclination 23.5°. While if we took the inclination of satellite in equatorial orbit, for example 10° note that the effect of the moon and sun with a date variable and this is what we have done in practice where the domain is not allowed to view all the results.

Figure (28) shows that the semi major axis (a) at hp=20000 (km) increases with time, the variation is(Δa =1.004223295555781km)

Figure (25)shows that the eccentricity (e) decreases with time. The change for altitude hp=20000 (km) (Δe=0.99953) and the variation is secular . Figure (27) shows the variations of mean anomaly that has the similar behavior due to SRP . Figure (29)shows the change of argument of perigee ($\Delta\omega$=0.9675569deg) the change is secular and it remains constant through any one rotation. Also the figures show that the perturbations are various because the variation of orbital elements at high altitude.

From results of the effect of SRP and lunar attraction concluded:

a for low orbits less than 10,000 is decreases and between 10000 to 30000 km increases that means the size's orbit increase.

e Less and the orbit bulging and approaching the spherical shape, slightly decreases at altitudes less than 30,000,and decreases faster during one period at high altitudes also there is small

difference about 0.00001 between variation of SRP and lunar gravity when medium and high altitudes**.**

i , Ω increases through 20 periods due to SRP and decreases due to lunar gravity and the values of change due to SRP larger than lunar attraction for altitude 20000 km where the acceleration of SRP larger than lunar gravity .

References

1. Kozai, Y.**1959**. On the Effect of the Sun and the Moon upon the Motion of a Close Earth Satellite. Smithsonian Astrophysical Observatory, Special Report 22, Cambridge, MA.
2. Musen, P.**1960**. The influence of the solar radiation pressure on the of an artificial satellite. J Geophys Res. 65:1391.
3. Musen, P. Bailie, A. and Upton, E. **1961**. Development of the Lunar and Solar Perturbations in the Motion of an Artificial Satellite. NASA-TN,D494.
4. Kozai, Y. **1961**. Spec. Repr. Smithsonian Inst., Astrophys. Obs., 25.
5. Kaula, M. W. **1962**. Development of the Lunar and Solar Disturbing Functions for a close satellite astronautical journal, 67, pp:300.
6. Radzievskii, V. V. and Arte'ev, A. V.**1962**. The influence of solar radiation pressure on the motion of artificial Earth satellites. Journal of Soviet Astronomy ,5, pp: 758.
7. Adams, W. M. Jr. and Hodge, W. F. **1965**. Influence of solar radiation pressure on orbital eccentricity of a gravity-gradient-oriented lenticular satellite. NASA-TN D-2715.
8. Sehnal,L. and Giacaglia,T. Ed. **1975**. Satellite Dynamics.Berlin,New York. Springer- Verlage.
9. Anselo, L. Bertotti, B. Farinella, P.Milani, A. and Nobili, A. M. **1983**. Orbital Perturbations Close Satellite. Journal of Astronautical, 67, pp:300.
10. Buffet, A. **1985**.short arc orbit improvement of GPS satellite. M.Sc. Thesis. Department of Geodesy and Geomatics Engineering, University of Calgary, Calgary, Canada.
11. Broucke, R. A. **1992**.The Double Averaging of the third Body Perturbations. Texas University, Austin, TX.
12. Kubo-oka, T. and Sengoku, A. **1999**.Solar radiation pressure model for the relay satellite of SELENE. Journal of Earth Planets Space, 51, pp: 979-986.
13. Su,H.**2000**.Orbit determination of IGSO, GEO and MEO satellites. Ph.D. Thesis. Department of Geodesy, University of Bundeswehr, Munchen, Germany.
14. Solórzano, C. R. H. and Prado, A. F. B. A. 20**0**4. Third-body perturbation using a single averaged model. Instituto Nacional de Pesquisas Espaciais – INPE, São José Campos, SP, Brazil, ISBN 85-17-00012-9.
15. Costa, I. V. and Prado, A. F. B. A. **2010**. Orbital evolution of a satellite perturbed by a third-body. Instituto Nacional de Pesquisas Espaciais- São José dos Campos-SP-12227-Brazil.
16. Lara, M. San-Juan, J. F. López, L. M. and Cefola, P.J. **2012**. On the third-body perturbations of high-altitude orbits. Celestial Mechanic Dyn. Astr. 113,pp:435-452.
17. Rahoma, W. A. and Metris, G.**2012**. Invariant Relative Orbits Taking into Account Third-Body Perturbation. journal of Applied Mathematics,pp:113-120. http://www.SciRP.org/journal/am.
18. Bar-Sever, Y. and Kuang, D. **2005**. New Epirically Derived Solar Radiation Pressure Model for Global Positioning System Satellites During Eclipse Seasons. IPN Progress Report 42-160 February 15.
19. Eshagh, M. and Najafi, A. M.**2007**. Perturbations in orbital elements of a low earth orbiting satellite. Journal of the Earth & Space Physics, 33(1),pp: 1-12.
20. Valk, S. and Lemaître, A. **2008**. Semi-analytical investigations of high area-to-mass ratio geosynghronous space debris including Earth's shadowing effects. Journal of Advances in Space Research, 42(8), pp:1429-1443.
21. Kezerashvili, R. Ya. and V'azquez-Poritz, J.F.**2009**,Solar Radiation Pressure and Deviations from Keplerian Orbits arXiv: gr-qc/0901.1606v2.
22. McMahon, J. and Scheeres, D.**2010**. The Secular orbit variation due to solar radiation effects: a detailed model for BYORP. Celest Mech Dyn Astr., 106, pp:261-300.
23. Khalil, K. I. and Ismail, M. N. S. **2011**. Effects of radiation pressure and Earth's oblatness on high altitude artificial satellite orbit. Journal of Astronomy Studies Development, 1:e1.
24. Sun, R. Zhao, C. Zhang, M. and Hou, Y.**2013**. Dynamical evolution of high area-

to-mass ratio object in Molniya orbits. Journal of Advances in Space Research, 51,pp:2136-2144. www.sciencedirect.com.

25. Zhou, Y. F. **2003**. A study for orbit representation and simplified orbit determination methods. M.Sc. Thesis. Queensland University of Technology, Australia.

26. Montenbruck, O. and Gill, E. **2001**. Satellite Orbits Models Methods And Applications. 2nd Edition, Springer–Verlag Berlin Heidelberg, Printed in Germany.

27. Meeus, J.**1988**. Astronomical Formulae For Calculation. 4th Edition, Willmann-Bell. Inc., Printed in the United States of America.

28. Seeber, G.**2003**. Satellite Geodesy. 2nd completely revised and extended edition, Walter de Gruyter. Berlin. New York.

29. Rim, H. J. and Schutz, B. E. **2001**. Precision orbit determination (POD). Geoscience laser and altimeter satellite system, University of Texas, United States of America.

30. Hardacre, S. **1996**. Control of collocated geostationary satellites. Ph.D. Thesis. College of aeronautics, Cranfield University.

31. Muees, J. **1991**. Astronomical Algorithms. Willmann-Bell Inc. ISBN 0-943396-35-2.